The Influence of Asperities, Joint Topology and Stress on Fracture Geomechanical Properties

Packulak, T.R., Ahmed Labeid M.T., Bonneau, D.A., Diederichs, M.S., Hutchinson, D.J.
Department of Geological Sciences and Geological Engineering, Queen's University, Kingston, ON, Canada

Day, J.J.
Department of Earth Sciences, University of New Brunswick, Fredericton, NB, Canada

ABSTRACT
Joint roughness directly affects the behaviour of discontinuities at the laboratory scale and the rockmass at the excavation scale. For the design of large underground infrastructure projects (e.g. deep base tunnels for transportation and deep geological repositories for the storage of nuclear waste), laboratory testing is required to measure geomechanical properties (e.g. strength and stiffness) for input to numerical models. This paper presents an analysis of the influence of joint surface topology and confining stress on joint strength and joint stiffness from direct shear testing. Joint topology is analyzed using Structure-from-Motion photogrammetry models of drill core specimens and used to discuss the influence on joint strength and stiffness. Joint topology was found to influence joint stiffness at lower confining stress conditions with decreasing influence as the confining stress increases. Finally, the effect of applied stress is discussed with implications for joint stiffness and joint strength.

RÉSUMÉ
La rugosité des joints affecte le comportement des discontinuités, soit à l'échelle du laboratoire, soit de l'excavation. Des tests en laboratoire sont requis pour déterminer les propriétés geomècaniques, comme par exemple, la résistance à la compression et la rigidité, des massifs rocheux, pour créer les modèles numériques, pour la conception des projets d'infrastructures souterrainnes (par exemple, le stockage en couches géologiques profondes pour la gestion de déchets nucléaires). Cet article analyse l'influence de la rugosité et de la topologie des joints, sous des conditions de contraintes pendant des essais de cisaillement, sur les caractéristiques des joints. La topologie des joints est caractérisée par l'utilisation des modèles Structure-from-Motion photogrammétriques. Il a été etabli que la rigidité des joints est influencée par leur topologie quand les conditions de contraintes sont plus basses, et que cette influence est reduite quand les conditions de contraintes sont plus élevées. Finalement, les implications de l'effet du stress appliqué sur la résistance à la compression et la rigidité des joints sont discutées.

1 INTRODUCTION

A rockmass is composed of two components: intact rock and discontinuities. The geomechanical properties of discontinuities, commonly referred to as rock joints, include deformability, strength, and dilation. These properties govern the joint and overall rockmass behaviour around rock engineering projects such as natural slopes, surface excavations, and underground infrastructure such as tunnels or caverns.

Laboratory testing is a more economical and practical method to measure geomechanical properties when compared to in situ testing. Measurements at the laboratory scale can then be applied to models at the excavation scale. However, one of the main limitations of laboratory testing is that tested specimens are significantly smaller than the rockmass system that is typically under investigation. In direct shear testing, geomechanical properties that are used as numerical modelling input parameters include: joint normal stiffness (K_n), joint shear stiffness (K_s), shear strength (τ), and dilation angle (ψ).

The topology or degree of roughness of a discontinuity directly affects the shear strength characteristic of the discontinuity. The degree of roughness of discontinuities has been incorporated into multiple constitutive models (Patton 1966; Barton and Bandis 1990). In rock engineering, one of the standard methods to describe the degree of roughness is the Joint Roughness Coefficient (JRC) (Barton and Choubey 1977). Visual comparisons of rock specimens to the standard roughness profiles can be subjective based on a user's level of experience (Beer at al. 2002; Stigsson 2018). To remove individual bias from visual interpretation, several quantitative approaches have been developed to assess roughness through statistical (Myers 1962; Tatone and Grasseli 2010) and fractal (Kulatilake et al. 2006) methods.

This paper integrates Structure-from-Motion (SfM) photogrammetry and a series of direct shear tests to assess the effects of joint roughness on geomechanical fracture properties. The influence of joint roughness, derived from SfM photogrammetry models, is assessed with respect to joint stiffness as well as shear and residual strengths using natural fractures of varying roughness and saw cut fractures as control specimens.

2 JOINT ROUGHNESS QUANTIFICATION

Given the well documented implications of joint roughness on the shear behaviour of discontinuities, multiple methods have been proposed to quantify joint roughness. These can be categorized as empirical methods (e.g. Joint Roughness Coefficient (JRC)), statistical methods (e.g.

center line average and average inclination), fractal methods, and signal analysis (e.g. Fourier Transformations).

The most popular empirical method to describe the surface roughness of a fracture is the JRC. The JRC value ranges from 0 for very smooth, planar joints to 20 for very rough, stepped joints. JRC values can be back calculated from direct shear tests, or visually estimated by comparing a joint surface to the set of 10 standard profiles (Barton and Choubey 1977; ISRM 1978).

There are multiple statistical parameters that can be used to describe surface roughness, including center-line average asperity height, root mean square asperity height, average asperity inclination, and others. These statistical parameters can be separated into two categories (Reeves 1985): parameters describing (i) the magnitude of the roughness, and (ii) the texture of the rough surface.

The quantification of roughness of a specific profile can also be assessed using fractal geometry. The use of fractals was first introduced by Mandelbrot (1967) to describe irregular shapes that appear to be random. The concept of fractional "dimension" (D) was introduced by Mandelbrot (1977) as a method of describing the complexity of a fractal object, and ranges between 1 for a flat line and 2 for 2-Dimensional (2D) profiles. The D values for rock joints are typically between 1 and 1.5 for 2D profiles (Tatone 2009).

Standard practice for describing joint roughness is JRC, as defined by both the original (ISRM 1978) and revised (Muralha et al. 2014) ISRM suggested methods for the quantitative description of discontinuities in rockmasses. Each method described in this section has undergone validation against the JRC standard profiles.

3 DETERMINATION OF GEOMECHANICAL FRACTURE PROPERTIES

Constant normal stress (CNL*) direct shear tests are completed in two stages: a normal loading stage and a shearing stage, which begins once the target normal stress has been reached, as shown in Figure 1.

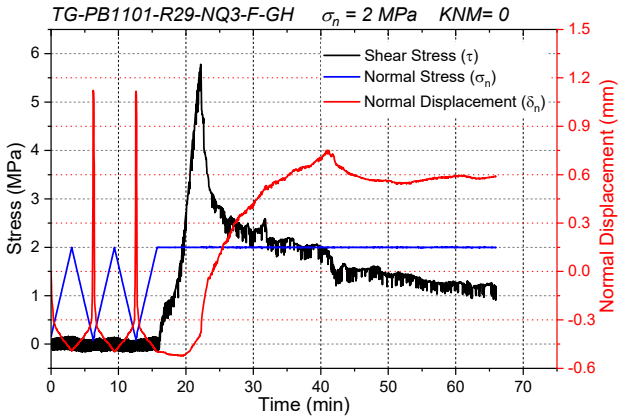

Figure 1. Full CNL* direct shear test: 0-15 minutes shows 3 normal loading cycles; 15-65 minutes shows the shear loading stage of the test

In direct shear testing, the normal and shear stiffness of a discontinuity is calculated using displacement and stress data prior to yielding. Normal stiffness is measured during the initial normal loading stage of the test. In order to describe the deformation during normal loading, multiple closure laws have been developed including a non-linear hyperbolic relationship (Goodman 1974), a semi-logarithmic relationship (Bandis et al. 1983), and a linear closure relationship (Hungr and Coates 1978).

Joint shear stiffness is measured near the beginning of the shear loading stage prior to yield. The joint shear stiffness is measured as the slope of the linear-elastic portion of the shear stress data with respect to shear displacement. Two methods are commonly used to measure joint shear stiffness: the yield (secant) method (Goodman 1970) and the yield (tangent) method (Hungr and Coates 1978). Secant shear stiffness is the secant between zero and yield shear stress, and tangent shear stiffness is the slope at 50% (approximated by a linear slope between 40% and 60%) of yield shear stress. In some direct shear tests, sample seating occurs, creating non-linear behaviour at the start of the test, which may be included by both the secant and tangent shear stiffnesses. To overcome this limitation, Day et al. (2017) introduced the best-fit chord approach, which involves manual selection of the pre-yield linear-elastic portion of the shear stress versus shear displacement curve. All shear stiffness measurement types are shown in Figure 2.

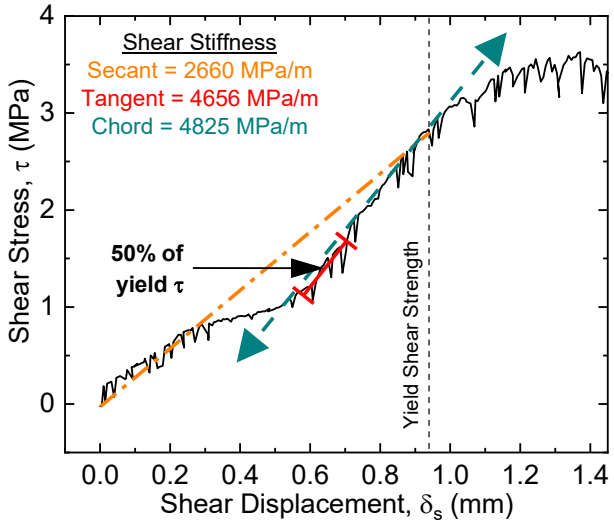

Figure 2. Detail view of shear stiffness measurements which include Secant (Goodman 1970), Tangent (Hungr and Coates 1978), and Best Fit Chord (Day et al. 2017)

Two distinct strength envelopes are typically determined from a direct shear test: a yield and residual strength envelope. Yield shear strength corresponds to the maximum shear strength of the specimen before dilation starts to occur. The residual shear strength is the sustained shear resistance of the failure surface after yield.

4 SURFACE ANALYSIS AND DIRECT SHEAR TEST RESULTS

The rock joint specimens used in this study are a combination of smoothly ground saw cut surfaces, machine breaks that formed during drilling, and natural fractures through NQ (47.6 mm diameter) and NQ3 (45 mm diameter) size drill core of gneissic tonalite, pink granite, and leucogranite units from the Canadian Winnipeg River Complex within the Pointe Du Bois Batholith (Figure 3).

The tonalites and granites are equigranular, medium to coarse grained, and are unfoliated to weakly foliated. The joints are smooth to semi-rough, planar to sub-planar, and are generally fresh with trace mineral coating. Machine breaks and naturally occurring joints were distinguished by the characteristics of the fracture: natural joints typically had a trace mineral coating of calcite or iron oxide, while machine breaks had rough, irregular profiles and fresh fracture faces.

Figure 3. NQ3 (45 mm) Pointe Du Bois core: (left) saw cut specimen, and (right) fracture specimen

Sample preparation and testing procedures for saw cut specimens are outlined by Ahmed Labeid et al. (2019). Sample preparation and testing guidelines for natural fractures are outlined by Day et al. (2017).

4.1 Structure-from-Motion Photogrammetry and Surface Analysis

Structure from Motion (SfM) photogrammetry is the process of generating 3-Dimensional (3D) point clouds from a series of overlapping photographs. SfM differs from traditional photogrammetry in that precise knowledge of the 3D location and orientation of the cameras are not required as an input to reconstruct scene geometry. SfM algorithms solve for the 3D location and orientation of the cameras, which results in a model that lacks an inherent scale. In order to georeference and apply a scale to the model, a series of ground control points (GCPs) are used, allowing the model to be used for further analysis. For further details on SfM photogrammetry, readers are referred to Smith et al. (2016).

In this study, each drill core specimen used in the analysis was placed at the center of a rotating table that was divided into 16 equal azimuth angles. Between 16 and 20 photographs of each sample were taken at different azimuth angles, focusing on the joint surface, using a Canon 70D DSLR camera with a 50 mm prime lens. To generate the 3D models, photographs were imported into Agisoft PhotoScan Professional V1.3.2 software (Agisoft LLC 2018). Two CGPs were used to scale and orient the photogrammetry models.

The dense point clouds generated in Photoscan were imported into the open-source software package CloudCompare (CloudCompare 2018). The point cloud was manually segmented so that only the joint surface of the sample remained.

In order to analyze the joint surface, the point cloud was imported into MATLAB (Mathworks 2018) and translated into Cartesian coordinates. The point cloud was then discretized into profiles with a width of two times the average point spacing along the X and Y axes. Approximately 400 profiles were generated across the width of the sample in each orientation. The average asperity angle and joint roughness coefficient were calculated for all profiles with a length greater than one-third of the central diameter of the specimen. This process was repeated at 10 degree increments to fully characterize the joint surface. For computational efficiency, profiles were generated in both the X and Y direction at each increment. The JRC was calculated using the Fourier approach as presented by Pickering and Aydin (2016).

The discontinuity surfaces and shear testing directions are shown in Figure 4 for fracture specimens. The JRC and average asperity angle, in relation to profile orientation, are shown in Figure 5.

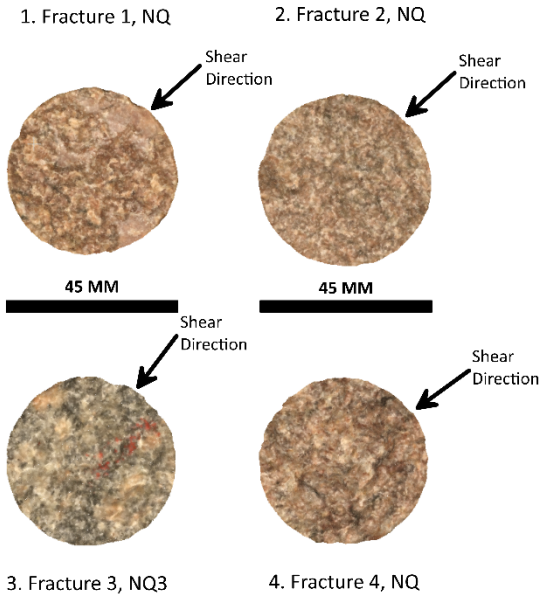

Figure 4. Photogrammetry surface models with shear directions marked

4.2 Pre-Yield Deformation Behaviour: Stiffness

To estimate joint normal stiffness (K_n), all test results from the normal loading stage (zero shear load) were analyzed using the linear (Hungr and Coates 1978) closure relationships between normal displacement and normal stress. Normal stiffness results for all the Pointe du Bois Batholith fracture samples range from 2,000 to 20,000 MPa/m. For saw cut samples, the joint normal stiffness (K_s) ranges from 4,000 to 10,000 MPa/m (Figure 6).

1. Fracture 1, NQ, n_{ave}=1342

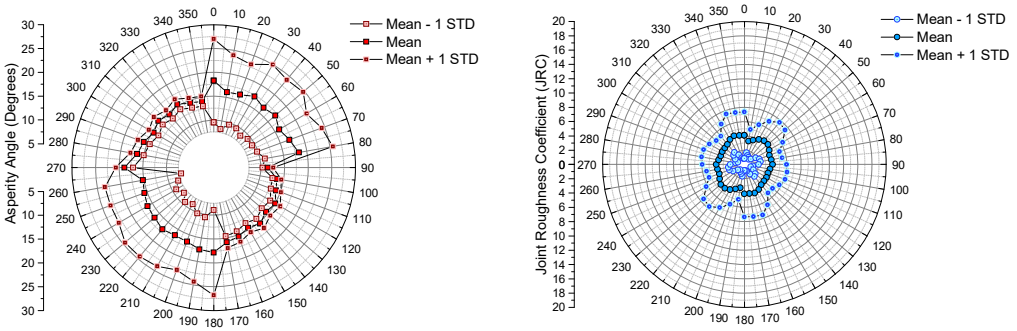

2. Fracture 2, NQ, n_{ave}=1365

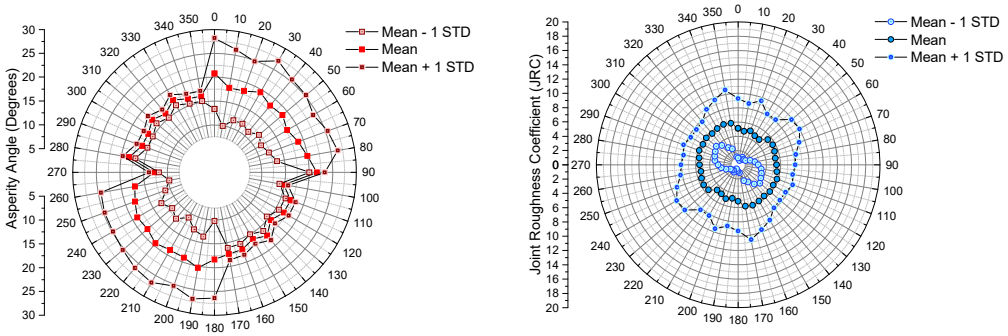

3. Fracture 3, NQ3, n_{ave}=652

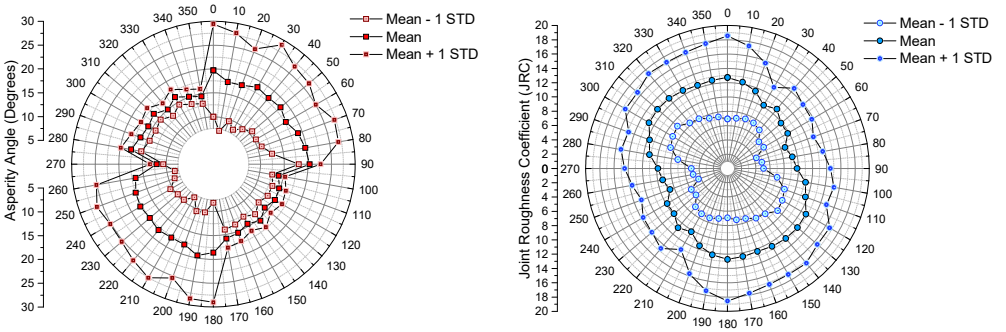

4. Fracture 4, NQ, n_{ave}=1269

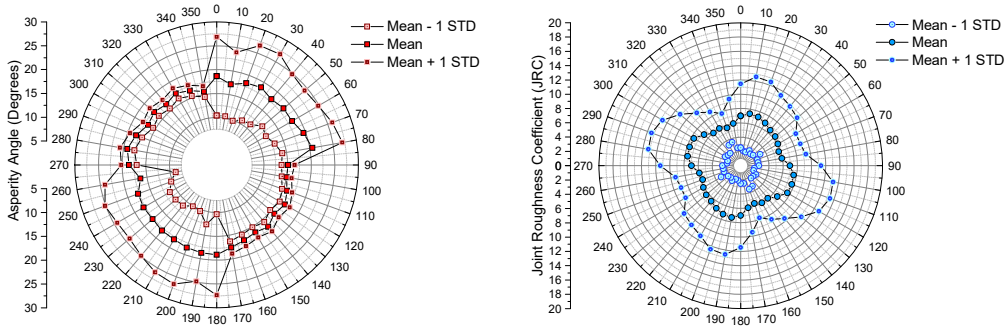

Figure 5. (Left) Calculated average asperity angle, and limits ±1 standard deviation (STD) for each specimen; (right) calculated average JRC and limits ±1 STD; the average number of profiles used in the statistical analysis at each directional increment is noted by the n_{ave} value for each specimen

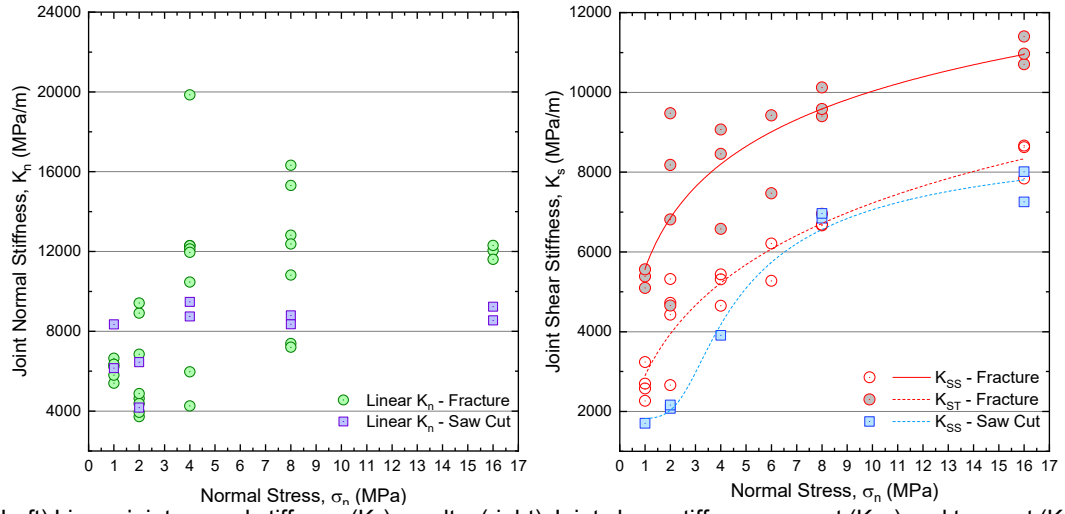

Figure 6. (Left) Linear joint normal stiffness (K_n) results; (right) Joint shear stiffness, secant (K_{SS}) and tangent (K_{ST}) results, non-linear curves are best fits of the Carreau-Yasuda rheological model.

Joint shear stiffness values were determined using the secant (K_{SS}) and tangent (K_{ST}) methods. The joint shear stiffness for fractures ranges from 2,000 to 9,000 MPa/m when analyzed using the secant method and 4,000 to 12,000 MPa/m when using the tangent method. Saw cut surfaces were only analyzed using the joint shear stiffness secant method, and values range from 1,000 to 8,000 MPa/m. Joint shear stiffness results for all specimens are shown in Figure 6. Joint shear stiffness and joint normal stiffness results of specimens tested in CNL* at a normal stress (σ_n) of 2 MPa, which correspond to the specimens analyzed using SfM photogrammetry for surface roughness (Figure 5), are listed in Table 1.

Table 1. Joint shear stiffness (K_{SS}) and joint normal stiffness (K_n) for specimens tested in CNL* at σ_n of 2 MPa

Specimen Name	K_{SS} [MPa/m]	K_n [MPa/m]
Saw Cut 1, NQ	2076	4177
Saw Cut 2, NQ	2161	6455
Fracture 1, NQ	2660	5560
Fracture 2, NQ	4427	8345
Fracture 3, NQ3	4723	5008
Fracture 4, NQ	5321	7339

4.3 Yield and Post Yield Behaviour: Shear Strength

Fractures and saw cuts tested under CNL* conditions show two failure envelopes for yield strength and residual strength. The yield and residual shear stress measurements for several tests can be plotted in normal stress versus shear stress space. When samples are tested at multiple normal stresses, failure envelopes can be fit to the test data in order to determine parameters for various strength criteria for engineering and numerical modelling purposes. In this study, the Mohr-Coulomb failure criterion (Coulomb, 1776) was used to fit the direct shear test data and define a cohesion value and friction angle, as shown in Figure 7. The results for specimens tested at 2 MPa (which correspond to those in Figure 5 and Table 1) are listed in Table 2.

Table 2. Summary of yield and residual shear strength for specimens tested in CNL* at σ_n of 2 MPa

Specimen Name	Yield Shear Strength τ_y [MPa]	Residual Shear Strength τ_r [MPa]
Saw Cut 1, NQ	1.3	-
Saw Cut 2, NQ	1.25	-
Fracture 1, NQ	3.6	2.3
Fracture 2, NQ	5.0	1.6
Fracture 3, NQ3	5.8	1.2
Fracture 4, NQ	7.1	2.3

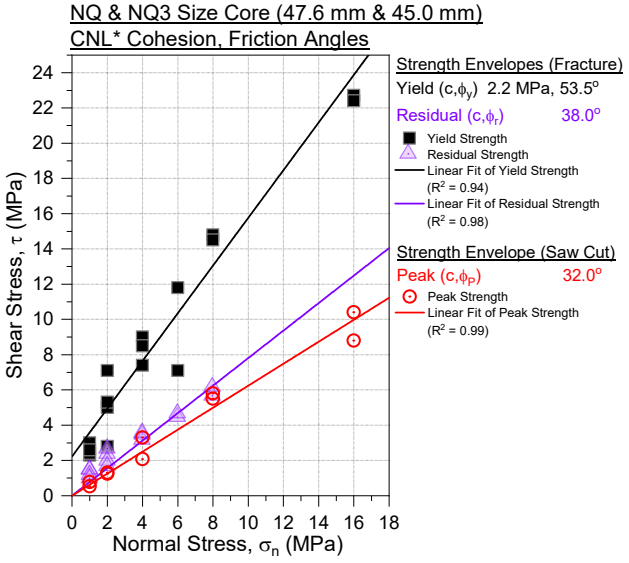

Figure 7. Shear strength results and Mohr-Coulomb strength envelopes of fracture and saw cut specimens in the CNL* boundary condition

5 DISCUSSION

Historically, the investigation of rock joints gained increasing importance in geotechnical design as it became evident that discontinuities governed the behaviour of rockmasses under low stress conditions. Recent advances in numerical modelling make it possible to simulate increasingly complex rockmass behaviour.

All joints, in general terms, have a degree of roughness, whether it is characterized by low angled undulations or sharp, high angled asperities. Previous research shows that this degree of roughness has an effect on the overall geomechanical behaviour of fractures (Patton 1966; Barton and Bandis 1990). Specifically, in the cases of Patton (1966) and Barton and Bandis (1990), the degree of roughness was proven to directly affect the shear strength of the discontinuity, which led to the development of constitutive strength models. These strength models typically have two components: (i) the base friction angle of the rock, found by conducting saw cut tests, and (ii) a term that quantifies the increase in shear resistance from joint asperities.

One important aspect that has not been sufficiently addressed is the influence of asperities on the deformation behaviour of fractures (stiffness). In this study, saw cut specimens are used as a base case in order to estimate the normal and shear stiffness during a direct shear test of a smooth plane. This data is compared to the direct shear data from four specimens of varying roughness ranging from JRC = 4 to JRC = 14.

Joint normal stiffness was examined in a numerical study by Hopkins et al. (1990) in which surfaces of varying contact area size were modelled to assess elastic deformation. Based on the theory of elasticity (Timoshenko and Goodier 1951), joints with smaller asperities were found to be stiffer than joints with larger asperities. As normal stiffness is function of spatial geometry and surface roughness, surfaces that form small dispersed contact are much stiffer than joints where the contact joints are large or comprised of large clusters of joints (Hopkins et al. 1990). Based on the results presented in Figure 6, at 2 MPa the linear joint normal stiffness ranges from 4,000 to 8,500 MPa/m. At the lower end of this range, the smoother joints with lower mean JRC values act in a similar manner to saw cut fractures, as there is a larger contact area when the stress is applied than rougher fractures.

In contrast to joint normal stiffness, the joint shear stiffness appears to be dependent on normal stress up to 8 MPa, but this dependence decreases with increasing additional normal stress. At a critical stress level, the joint will reach maximum closure and will be fully mated, as asperities are confined and joint opening cannot occur. As a result, joint shear stiffness will most likely be dependent on the intact material stiffness and not on the asperities or applied stress.

Based on the results shown in Figure 5 and Figure 6, some of the variability in joint normal stiffness may be due to joint roughness; however, it is uncertain to what degree joint normal stiffness is dependent on joint topology. The measurement of joint normal stiffness has been shown to be sensitive to testing technique and apparatus as non-linearity in some tests have been attributed to sample seating (Goodman 1976; Day et al. 2017).

In agreement with previous studies, shear strength displays a strong dependency on joint roughness. Samples with higher JRC values exhibit higher shear strengths. This is exemplified by some fracture samples that exhibit higher residual strengths than the saw cut samples (Figure 7). Residual strength for these direct shear tests were typically measured after 5 mm of shear displacement and the fractures may not have been fully damaged. Based on the listed yield strength values in Table 2, Fracture 3 has the highest average JRC value (Figure 5) but does not have the highest strength. This specimen from the Pointe Du Bois Generating Station is a different lithology than Fractures 1, 2, and 4 with minor differences in crystal size and mineralogy (Packulak 2018). Fractures 1, 2, and 4 are pink granite with relatively coarse grained felsic minerals of a consistent size. Specimen 3 is the mafic member of the tonalite gneiss and has a bimodal crystal size distribution where the feldspar crystals are quite large with distinct cleavage planes. These geologic features may facilitate premature failure due to mineral grain orientation. Alternatively, based on the overall large crystal size in Fracture 4, the shear strength may be more influenced by the strength of a single crystal instead of the joint surface as a whole.

Based on the results of the asperity angle analysis (Figure 5), there does not appear to be any correlation with average asperity angle and geomechanical properties (strength and stiffness). In a typical direct shear test, not all asperities contribute to the fracture behaviour. It is recommended that further study be conducted to analyze individual areas of broken asperities in order to confirm the degree to which asperity angle and/or height may influence geomechanical properties.

6 CONCLUSIONS

The research presented in this paper covers concepts that pertain to the estimation of discontinuity geomechanical properties using saw cut samples and natural fractures. The primary conclusions of this paper are summarized below:

- Normal stiffness is not dependent on stress; however, at low stresses, variability in normal stress measurements is dependent on joint topology. At higher stresses, variability is minimal.
- Shear stiffness is dependent on normal stress at stresses <8MPa. At low stress values, the shear stiffness is variable due to specimen seating, topology and stress. At stresses >8MPa, variation in shear stiffness is reduced and the dependence on stress is minimized.
- It is unclear how sensitive geomechanical properties are to asperity angle. The mean asperity angles for all specimens were relatively similar and further research is warranted to isolate and analyze individual broken asperities.
- Geomechanical properties of samples at the laboratory scale (NQ (47.6mm) and NQ3 (45mm))

appear to be dependent on the deformation and strength of individual crystals.

7 ACKNOWLEDGMENTS

The Natural Sciences and Engineering Research Council of Canada and the Canadian Nuclear Waste Management Organization have financially supported this research. Thanks to Manitoba Hydro and KGS Group Consulting Engineers for supplying the rock core samples.

8 REFERENCES

Agisoft LLC. 2018. Agisoft PhotoScan Professional (Version 1.3.2). Available from http://www.agisoft.com/downloads/installer/.

Ahmed Labeid, M.T., Dossett, W.C., Day, J.J., and Diederichs, M.S. 2019. Investigation of the Mechanisms of Stick-Slip Behaviour in Smooth Granite Joints. *In Proceedings of the 14th Congress of the International Society of Rock Mechanics*. Foz do Iguassu, Brazil. p. 8.

Bandis, S.C., Lumsden, A.C., and Barton, N.R. 1983. Fundamentals of rock joint deformation. *International Journal of Rock Mechanics and Mining Sciences & Geomechanics Abstracts,* 20(6): 249–268.

Barton, N., and Bandis, S.C. 1990. Review of predictive capabilities of JRC-JCS model in engineering practice. I*n Proceedings of the International Symposium on Rock Joints.* Edited by N. Barton and O. Stephansson. A.A. Balkema, Loen, Norway. pp. 603–610.

Barton, N., and Choubey, V. 1977. The shear strength of rock joints in theory and practice. *Rock Mechanics*, 10(1–2): 1–54.

Beer, A.J., Stead, D., and Coggan, J.S. 2002. Technical Note Estimation of the Joint Roughness Coefficient (JRC) by Visual Comparison. *Rock Mechanics and Rock Engineering,* 35(1): 65–74.

CloudCompare. 2018. CloudCompare (Version 2.10-alpha). Available from http://www.cloudcompare.org/.

Coulomb, C.A. 1776. Esai Sur Une Application res degeles des Maximum et Minimis des Stalique Relations a L'Architecture. *In Mémoires de mathématique et de physique, presentés à l'Académie royale des sciences, par divers sçavans & lûs dans ses assemblées.* Paris. pp. 343–387.

Day, J.J., Diederichs, M.S., and Hutchinson, D.J. 2017. New direct shear testing protocols and analyses for fractures and healed intrablock rockmass discontinuities. *Engineering Geology,* 229: 53–72.

Goodman, R.E. 1970. The Deformability of Joints. In *Determination of the In Situ Modulus of Deformation of Rock.* Edited by Committee D-18. ASTM International, West Conshohocken, PA. pp. 174–196.

Goodman, R.E. 1976. *Methods of Geological Engineering in Discontinuous Rocks*, West Publishing Company, St. Paul, MN, United States of America.

Hopkins, D.L., Cook, N.G.W., and Myer, L.R. 1990. Normal Joint Stiffness as a Function of Spatial Geometry and Surface Roughness I*n Proceedings of the International Symposium on Rock Joints.* Edited by N. Barton and O. Stephansson. A.A. Balkema, Loen, Norway. pp.203-210.

Hungr, O., and Coates, D.F. 1978. Deformability of joints and its relation to rock foundation settlements. *Canadian Geotechnical Journal*, 15(2): 239–249. doi:10.1139/t78-022.

International Society for Rock Mechanics. 1978. Suggested methods for the quantitative description of discontinuities in rock masses. International Journal of *Rock Mechanics and Mining Sciences & Geomechanics Abstracts*, 15(6): 319–368. doi:10.1016/0148-9062(78)91472-9.

Kulatilake, P.H.S.W., Balasingam, P., Park, J., and Morgan, R. 2006. Natural rock joint roughness quantification through fractal techniques. *Geotechnical and Geological Engineering*, 24(5): 1181–1202.

Mandelbrot, B. 1967. How Long Is the Coast of Britain? Statistical Self-Similarity and Fractional Dimension. *Science,* 156(3775): 636–638.

Mandelbrot, B.B. 1977. *Fractals: form, chance, and dimension.* Freeman, San Francisco.

Mathworks Inc. 2018. MATLAB (Version R2018B). Available from http://www.mathworks.com.

Muralha, J., Grasselli, G., Tatone, B., Blümel, M., Chryssanthakis, P., and Yujing J. 2014. ISRM suggested method for laboratory determination of the shear strength of rock joints: revised version. *Rock Mech Rock Eng*, 47(1): 291-302.

Myers, N.O. 1962. Characterization of surface roughness. *Wear*, 5(3): 182–189.

Packulak, T.R.M. 2018. Laboratory Investigation of Shear Behaviour in Rock Joints Under Varying Boundary Conditions, M.A.Sc. Thesis, Queen's University at Kingston, Kingston, ON, Canada

Patton, F.D. 1966. Multiple modes of shear failure in rocks. *In Proceedings of the 1st Congress of the International Society of Rock Mechanics*. Lisbon, Portugal. pp. 509–513.

Pickering, C. and Aydin, A. 2016. Modeling Roughness of Rock Discontinuity Surfaces: A Signal Analysis Approach. *Rock Mechanics and Rock Engineering*, 49(7): 2959-2965.

Reeves, M.J. 1985. Rock surface roughness and frictional strength. *International Journal of Rock Mechanics and Mining Sciences & Geomechanics Abstracts,* 22(6): 429–442.

Smith, M.W., Carrivick, J.L., and Quincey, D.J. 2016. Structure from motion photogrammetry in physical geography. *Progress in Physical Geography*: Earth and Environment, 40(2): 247–275.

Stigsson, M. 2018. Finally, an objective way to infer JRC from digitized fracture traces. *In Proceedings of the 52nd US Rock Mechanics/ Geomechanics Symposium.* American Rock Mechanics Association. Seattle, WA, USA. p. 6.

Tatone, B.S.A. 2009. Quantitative characterization of natural rock discontinuity roughness in-situ and in the laboratory. M.A.Sc. Thesis, University of Toronto

Timoshenko, S. and Goodier, J.N. 1951. *Theory of Elasticity*, McGraw-Hill Book Company (2nd ed.), New York, NY, United States of America.